Miles, M., M.A. Imam, and M. Fleischmann. *"Case Studies" of Two Experiments Carried Out With the ICARUS Systems*. in *8th International Conference on Cold Fusion*. 2000. Lerici (La Spezia), Italy: Italian Physical Society, Bologna, Italy

"CASE STUDIES" OF TWO EXPERIMENTS CARRIED OUT WITH THE ICARUS SYSTEMS

M. H. Miles,* M. A. Imam,** and M. Fleischmann***

*Naval Air Warfare Weapons Division, China Lake, CA 93555-6100, U.S.A.

**Naval Research Laboratory, Washington, D.C. 20375, U.S.A.

*** ENEA, Frascati Research Centre, 00044 Frascati, (Rome), Italy.

I. ABSTRACT.

The publication of the Final Report of the New Hydrogen Energy (N.H.E.) Group on their investigations of the Pd/D systems (1) prompts us to analyse a number of experiments carried out with the ICARUS Systems (2), (3). As the reproducibility of such experiments remains low, our analyses rely on a series of "Case Studies" which use appropriate parts of the methodologies developed for these systems (2), (3) (see) also (4), (5), (6), (7), (8).

In this paper we present selected parts of such "Case Studies for two experiments carried out in the N.H.E. Laboratories; full details will be given elsewhere (9). The first experiment, designated as FP2 - 9506203 - 5561 used a 2 mm diameter × 12.5 mm length Pd cathode supplied by the IMRA-Materials Laboratory; the second FP2-97120402-M7C2, was carried out by one of us (M.H.M.) also in the N.H.E. Laboratories. This experiment used a 4.75 mm diameter × 20.1 mm length Pd - 0.5%B cathode (prepared by M.A.I. in the Naval Research Laboratory, Washington, D.C.). Contrary to the conclusions reached in the N.H.E. report (1) we find that these experiments show "Heat-after-Death" and excess enthalpy generation at temperatures close to the boiling points of the electrolytes. The experiment using the Pd-B cathode also shows excess enthalpy generation in other temperature regions as well as the very early development of "positive feedback" (compare (10), (11), (12)). Such "positive feedback" complicates the analyses of the experiments. The "Case Studies" of these experiments also lead to the identification of errors in the execution and analyses of the experiments carried out by the N.H.E. Group.

2. EXPERIMENT DESIGN AND RESULTS.

In common with other experiments carried out in the N.H.E. Laboratories, measurements were made using an ICARUS-1 type Calorimeter illustrated schematically in Fig. 1. Figs 2 and 3 show respectively the "raw data" for an early stage and part of the final day of the measurement sequences for the experiment with the Pd-cathode; Fig 4 gives these data for the key day of operation of the experiment with the Pd-B cathode. We note that experiment FP 2-9506203-5661 has been carried out in accord with the instructions for the ICARUS Systems (2), (3) in that the

measurement cycles lasted 2 days. This allowed the use of calibration pulses of 12-hour duration (see Fig 2) leading to the complete relaxation of the temperature perturbations. However, the majority of the experiments carried out in the N.H.E. Laboratories used measurement cycles lasting just 1 day such as those illustrated in Fig 5.

Data acquisition was carried out with an ICARUS-2 type system (3). However, as far as experiment FP2-9506203-5661 is concerned, it appears that the software controlling the data acquisition computer has been rewritten because the times for measurements with the "short thermistor", Fig 1, do not coincide with those for the "long thermistor" (which themselves coincide closely with those for the measurements of the cell current, cell voltage and bath temperature). This change is not crucially important for the preliminary data analyses described in this paper (except for the loss of redundancy in the measurements and, especially, for the evaluation of the evaporation to dryness on Day 29 of the experiment) because the synchronised data are sufficient to allow such analyses. A more serious matter is the loss of synchronisation of the calibration pulses, Fig 5. In consequence, the data evaluation must be restricted to the differential heat transfer coefficients determined locally e.g. $[k_R']_{11}$ and $[k_R']_{12}$. [1] The more precise integral heat transfer coefficients (e.g. $[k_R']_{21}$ and $[k_R']_{31}$ and accurate integral heat transfer coefficients (e.g. $[k_R']_{22}$ and $[k_R']_{32}$) will have serious errors unless this loss of synchronisation is taken into account 9); this applies especially to the true heat transfer coefficient, $[k_R']_{32}$, which we believe has been used extensively in the interpretations carried out by the N.H.E. Group.

3 DATA EVALUATION FOR EXPERIMENT FP2-9506203-5661

3A. THE DIFFERENTIAL LOWER BOUND HEAT TRANSFER COEFFICIENTS FOR DAYS 5-26.

The first stage in the ICARUS data evaluation scheme is the examination of these coefficients, designated as $[k_R']_{11}$, and of the relevant 11-point means, $\left[\overline{k_r'}\right]_{11}$ of $[k_R']_{11}$ see e.g. (4), (5), (10), (11), (12). Here we assume initially that there is a zero rate of excess enthalpy generation, hence $[k_R']_{11}$ is a lower bound. The development of excess enthalpy generation is then shown by falls in $[k_R']_{11}$; conversely decreases in excess enthalpy generation are shown by increases in $[k_R']_{11}$; see e.g. (8). It will be evident that if there is no excess enthalpy generation (e.g. in suitable "blank" experiments), then $[k_R']_{11}$ will be identical to the true heat transfer coefficient, $[k_R']_{12}$, obtained by applying appropriate calibration pulses. We believe that this condition applies to the major part of experiment FP2-9506203-5661 viz. to Days 5 - 26 (9).

The coefficients $[k_R']_{11}$ discussed in this paper have been obtained in a second cycle of calculations where the first cycle leads to the water equivalent to be used in this second cycle. The need to use such a second cycle will be discussed elsewhere, (9); we note that this procedure does not appear to have been followed in the evaluations carried out by the N.H.E. Group.

We also note that the expected value of the water equivalent is in the range 450-460 JK^{-1} whereas the measured values are in the range 490-525 JK^{-1}. We take this increase to be due to

[1] $[k_R']$ is the heat transfer coefficient. The format is explained in Appendix A

the “overfilling” of the cells with electrolyte and/or D_2O which must have contained ~6 Moles of D_2O rather than the ~5 Moles as given in the instructions for the ICARUS Systems (2), (3). This “overfilling”, which is also indicated by the rise of $[k_R']_{11}$ for the initial stages of the measurement cycles, Fig 6 (see also (9)), must be taken into account in the analysis of the “evaporation to dryness” on Day 29 (see Section 3C below).

The lack of control in the replenishment of the D_2O content of the electrolyte is also shown by the variability of $[k_R']_{11}$ under nominally identical conditions. Thus the extrema of the behaviour for the polarisation carried out at a cell current ~0.5A shows a 0.36% change in $[k_R']_{11}$. This is outside the error limits specified for the ICARUS Systems.

Fig 6 shows that the derived values of $[k_R']_{11}$ vary with the cell current; we see also that these values are much larger than those calculated using the Stefan - Boltzmann coefficient and the radiant surface area (this is especially true of the values determined at the higher cell current). Furthermore, close inspection of the data on expanded scales, e.g. Fig 7, shows that there are changes in $[k_R']_{11}$ during the application of the calibration pulse, for $t_1 < t < t_2$, as compared to the behaviour for $t < t_1$ and $t > t_2$. All these facts show that either or both of the input enthalpies to the cell and heater are in error: the test for the absence of such effects has always been used for assessing the satisfactory execution of the experiments, (13). We believe that all these observations can be explained by power dissipation in the leads external to the cell due to the use of the wiring supplied for the ICARUS-1 Systems (2) to connect the cells to the ICARUS-2 VERSION (3). Fig 8A shows the effects of including an 1 Ohm lead resistance in the current leads external to the cell (this resistance is the median value of the lead resistances supplied with the ICARUS-I Systems). It is evident that the values of $[k_R']_{11}$ determined at the two cell currents are now in reasonable accord and, moreover, that these values are close to those predicted from the Stefan-Boltzmann coefficient and the radiant surface area. However, we also note that the errors introduced by the mismatch of the enthalpies delivered to the cell and heater now have the opposite sign to those in Fig 7. It is evidently necessary to correct also for power losses in the leads to the calibrating heater and Fig 8B shows the effects of including an 1 Ohm resistance in these leads. The offset seen in Fig 8A can be seen to be reduced; however, a complete cancellation of this offset requires us to assume a resistance of 2.5 Ohms in these leads, Fig 8C, and this particular value also removes the offsets throughout the measurement sequence. However, such an high value of the lead resistances is unlikely and it may well be therefore that the enthalpies delivered to the calibration heater were lower than those given in the “raw data” for this experiment. A further discussion of these particular aspects will be given elsewhere (9).

We note finally that the inclusion of the power dissipation in the external wiring in the enthalpy input to the cells leads to an overestimate of $[k_R']_{11}$ ~5% (and the raising of the errors in the precision of $[k_R']_{11}$ from 0.1 to 5%). It is possible that these errors are the principal cause of the observation that $[k_R']_{11}$ can exceed the true value of $[k_R']_{12}$ (1) although there are further factors which can lead to the underestimate of $[k_R']_{12}$ (9), (14).

The further discussion of this particular experiment given in this paper will be based on the uncorrected values of $[k_R']_{11}$ as the corrections of the “raw data” for unknown external resistances can hardly be justified (however, see Sections 3C and 3D).

3B. THE DIFFERENTIAL LOWER BOUND HEAT TRANSFER COEFFICIENTS FOR DAYS 27-28.

The operation of the cell on Days 27-28 has been excluded from Section 3A principally because $[k_R']_{11}$ shows a significant fall with time during this penultimate measurement cycle (9). Such decreases are due to the development of excess enthalpy generation as the cell temperature increases. However, Fig 9 shows that the derived values of $[k_R']_{11}$ now become sensitive to the atmospheric pressure (due to the sensitivity of the enthalpy of evaporation to this variable as the temperature increases). Unfortunately, it appears that the on-line pressure sensor supplied with ICARUS-2 was disconnected so that it is not possible to evaluate this measurement cycle with complete certainty. However, increases of $[k_R']_{11}$ with time can be excluded as the surface area available for heat transfer decreases with time (compare Fig 8). It follows that value of the atmospheric pressure $P^* > 1$ must be excluded. The atmospheric pressure which must have applied to the operation of the cell towards the end of Day 28 can be specified more closely by considering the evaporation to dryness on Day 29 (see Section 3C). The cell is driven to dryness at 23,000 s after the start of the measurement cycle and we can therefore determine the value of P^* required to achieve this condition at this time (9). This pressure lies between 0.975 and 0.980 Ats which thereby also determines the variation of $[k_R']_{11}$ with time, Fig 9.

3C ENTHALPY BALANCES AND RATES OF EXCESS ENTHALPY GENERATION FOR t < 23,000 s OF DAY 29

The most direct way of estimating these quantities is illustrated in the Tabulation, Fig 10, which gives directly the excess enthalpy required to achieve complete evaporation of the D_2O content of the electrolyte. If we assume that this is generated at a constant rate, we then arrive at a mean rate of excess enthalpy generation. It is important to realise that this calculation is quite independent of all the information required for the calculation of the time dependence of the rates of excess enthalpy generation, see the Tabulation in Fig 11, except for the need to specify the volume of electrolyte in the system (a minor correction required is that for the variation of the enthalpy of evaporation with concentration). The calculation has therefore been given for the nominal cell contents of 5 Moles as well as for 6 Moles of D_2O. We believe that the actual volumes are closer to the latter rather than the former figure in view of the evident “overfilling” of the cell.

It will be seen that the Table given in Fig 10 also contains a second estimate in which the enthalpy input to the cell has been corrected to allow for power dissipation in the external leads (see Section 3A) together with a correction to the heat transfer coefficients. The excess enthalpy terms are not markedly affected by these corrections i.e. the estimates are “robust”.

The simplicity of this calculation must be contrasted with the complexities of calculations of the variation of the rate of excess enthalpy generation with time, Fig 11. Such calculations have been carried out so far within the framework of “ideal solution theory” which may not be adequate for the concentrated electrolyte developed in the cell. Detailed calculations will be presented elsewhere (9); however, we note here that it is impossible to achieve a satisfactory interpretation of the evaporation to dryness for any plausible values of the reflux ratio while in the absence of reflux, the rates of evaporation require negative rates of excess enthalpy generation at long times,

a behaviour which is forbidden by the Second Law of Thermodynamics. We believe that these contradictions are due to errors in the concentration and volume of electrolyte. Furthermore, the "long thermistor" and Pd cathode may not have been in the positions shown in Fig 1 which are required to allow the evaluation of the data during evaporation to dryness.

In view of the uncertainties in the interpretation of the data at long times for Day 29, we have evaluated the rates of excess enthalpy generation shown in Fig 13 at times t < 10,000 s.

3D HEAT-AFTER-DEATH ON DAY 29 FOR t >23,700 s.

The cooling of cells following evaporation to dryness is possibly the simplest calorimetric experiment which can be devised for "Cold Fusion" Systems (4), (5), (15). There is now no thermal input to the cell and no evaporative cooling so that the interpretation of such experiments is especially straightforward.

Inspection of the cooling curve for t > 23,700 s, Fig 3, shows that this cannot possibly be explained by the cooling of an empty cell with the heat transfer coefficient which applies to such cells (15): the rate of cooling is too slow which can only be explained by enthalpy generation in the system. Fig 12 compares the behaviour derived from the cooling curve shown in Fig 1 with that predicted in the absence of excess enthalpy generation.

The rates of excess enthalpy generation can evidently be derived from the difference between the radiative output from the cell and the change in enthalpy content of the calorimeter. Fig 13 shows the relevant data and it appears that at t = 0 for the cooling curve (i.e. at 23,700 s) the rates lie between those calculated for the cell filled with electrolyte for P* = 0.985 and p* = 0.980 Ats. (see Section 3C).

4. DATA EVALUATION FOR EXPERIMENT FP2 - 47120902-M7C2.

Pd-B alloy electrodes of the type used in this experiment had been shown to give excess enthalpy generation in previous experiments (16), (17). An evaluation of the experiment discussed here but using a different methodology has also been presented at ICCF-8 (18) while full reports of the ICARUS -type analysis will be given elsewhere (9), (19), (20).

Comparison of the "raw data" for the experiment with the Pd-B cathode, Fig 4, with those for the Pd cathode, Fig 2, shows that the approach to the steady state is delayed for the former electrode following the application of the heater calibration pulse. This is an immediate indication of the onset of "positive feedback": an increase in the rate of excess enthalpy generation induced by the increase in the cell temperature, here due to the imposition of the calibration pulse (compare e.g. (12)). It is of special interest that such "positive feedback" develops at such an early stage of the experiment. However, it is not possible to determine at the present time whether this effect is a general feature of the use of Pd-B alloys.

The presence of "positive feedback" greatly complicates the evaluation of the data because it is not possible in general to calibrate "closed loop" systems in the presence of such feedback.

4A. THE N.H.E. EVALUATION

The Group at N.H.E. have quoted a single value of the "true heat transfer coefficient" $[k_R']_{12} = 0.793504 \times 10^{-9}$ WK^{-4}, on Day 3 of this experiment (i.e. for the data in Fig 4) and have used this value for all further evaluations. The magnitude of the calibration pulse, $\Delta Q \sim 0.2500W$ during $t_1 < t < t_2$ has also been excluded in the calculations; furthermore, the water equivalent 490 JK^{-1} contained in the original parameter listing for the ICARUS-Systems (2), (3) has been used throughout rather than to revise the value to that applicable to this experiment.

We arrive at the data shown in Fig 14 and can identify an immediate shortcoming of the procedure used by N.H.E.: it is not possible to determine whether $[k_R']_{11}$ during $t_1 < t < t_2$ falls on the same straight line as the values for $t < t_1$ and $t > t_2$ (compare Fig 7). Proceeding further with the N.H.E. style analysis we derive the rates of excess enthalpy generation shown in Fig 15. We can see that this evaluation must be subject to one or several errors. In the first place, it is not possible for the cell to be endothermic during $t_1 < t$ and $t > t_2$ as the endotherminity of the cell reaction has already been fully taken into account by using the thermoneutral potential. Secondly, we note that it has been maintained (21) that the N.H.E. methodology recovers the magnitude of the heater calibration pulse, ΔQ, during $t_1 < t < t_2$ together with any rate of excess enthalpy generation. Fig 15 shows that this is incorrect. The values of the rates of excess enthalpy generation are smaller than ΔQ if we fix the base-line at $Q_{excess} = 0$. If we fix the base-line excess at the level of the negative rate of excess enthalpy generation tor $t < t_1$ then $Q_{excess} > \Delta Q$ during $t_1 < t < t_2$. The methodology used by N.H.E. can, in fact, only be used under an highly restricted range of conditions which do not apply to this particular measurement cycle (14).

4B THE ICARUS-TYPE EVALUATION.

In view of the very early development of "positive feedback" we can only evaluate the "true heat transfer coefficient, $[k_R']_{12}$" at times close to t_1. Such an evaluation shows that $[k_R']_{12}$ must be at least 0.83808×10^{-9} WK^{-4} while the water equivalent, 454 JK^{-1}, is close to the expected value. Use of this value and inclusion of ΔQ in the enthalpy input to the cell gives the variation of $[k_R']_{11}$ with time shown in Fig 16. The fact that the application of the calibration pulse leads to a build up of excess enthalpy generation (and hence to a fall of $[k_R']_{11}$) can now be clearly seen: more complete discussions will be given in (9), (19) and (20).

In view of the intervention of "positive feedback", we are unable to apply the methodology for the evaluation of the "integral lower bound heat transfer coefficients, $[k_R']_{21}$ and $[k_R']_{31}$" as well as of the "integral true heat transfer coefficients, $[k_R']_{22}$ and $[k_R']_{32}$" in the manner set out in the Handbooks (2), (3). However, as the effects of "positive feedback" are relatively small and confined in the time-domain, Fig 16, we can include the additional rates of enthalpy input in the integral of the total enthalpy and evaluate the target "true integral heat transfer coefficient, $[k_R']_{352}$" as well as the water equivalent, Fig 17. We obtain the values $[k_R']_{352} = 0.85065 \times 10^{-9}$ WK^{-4}, water equivalent = 450 JK^{-1}. However, we note here that in general the coefficient $[k_R']_{252}$ based on the backward integration of the data sets, is to be preferred to $[k_R']_{352}$ which is based on forward integration (9), (14), (19), (20). In view of the fact that this evaluation of the "true heat transfer coefficient" requires a special approach, it is necessary (and advisable) to investigate

whether the value can be confirmed using other parts of the experiment. One such confirmation can be obtained from the initial parts of the experiment where the rate of any excess enthalpy generation must be small. In this region we can show that the maximum value of $[k_R']_{11}$ is closely similar to $[k_R']_{352}$ (9), (19), (20) (compare (4), (5)). A second confirmation can be obtained on Day 61 where we must again have a low rate of excess enthalpy generation (see Section 3C). In this case we find that $[k_R']_{11}$ agrees with the value of $[k_R']_{352}$ determined above together with the time-dependence of $[k_R']_{11}$ as given by appropriate "blank" experiments (8), (14).

4C. ADDITIONAL COMMENTS ON THE RATES OF EXCESS ENTHALPY GENERATION

Fig 18 gives the rate of excess enthalpy generation determined with the correct value of the "true heat transfer coefficient". The near zero value for $t < t_1$, the build-up due to "positive feedback" during $t_1 < t < t_2$ and the relaxation of this effect for $t > t_2$ can now be clearly seen.

Fig 19 gives the corresponding plot evaluated by analogy to the procedure used by the Group at N.H.E. The near zero rate for $t < t_1$, steps of Q = 0.25 W at $t = t_1$ and $t = t_2$, the build-up of excess enthalpy generation during $t_1 < t < t_2$ and the decay for $t > t_2$ are now evident.

Fig 20 gives the integrals of the rates of excess enthalpy production for the whole of the experiment when using the heat transfer coefficient determined by N.H.E. The large negative excess enthalpies are clearly not acceptable as they violate the Second Law of Thermodynamics.

Fig 21 gives a plot corresponding to Fig 20 but based on the true heat transfer coefficient evaluated in the present report. We can see that the negative excess enthalpies are now eliminated.

4D THE BEHAVIOUR ON DAY 68: EVAPORATION TO DRYNESS AND HEATAFTER-DEATH.

The analysis for the period $0 < t < 21{,}300$ s during which the cell is driven to dryness is similar to that presented in Section 3C and will be presented elsewhere (9), (14), (20). The analysis of the cooling curve for the period $21{,}300 \text{ s} < t < 86{,}400$ s is similar to that which has been given in Fig 12 except that it is necessary to allow for a low level of enthalpy input from the Galvanostat during the initial part of this period. Fig 22 shows the specific rates of excess enthalpy generation as the cell is being driven to dryness as well as during the observation of Heat-after-Death. As for the case of experiment FP-95062035661, Fig 13, it appears that the rates converge to a common value in the region where dryness is achieved

The full discussion of this experiment (9), (19), (20), will also comment on other periods during which it is possible to observe Heat-after-Death. This includes the period $2{,}400 \text{ s} < t < 32{,}400$ s during which the cell was disconnected from the Galvanostat and the period Day 25 + 76,300 s < t < Day 26 + 22,300 s during which there was a marked reduction in the cell current (the conditions follow Scenario 1 for the observation of Heat-after-Death (6), (7)). This period of operation is of special interest because the rate of excess enthalpy production exceeded the rate of enthalpy input to the cell.

5. CONCLUSION.

The two experiments used to illustrate this paper show all the features to which we have previously drawn attention: excess enthalpy production in Pd-based cathodes charged with deuterium, “positive feedback”, evaporation to dryness, Heat-after-Death. The results obtained contradict those reported by the group at N.H.E. and it is therefore important that this group should present a detailed evaluation of these (and other!) experiments.

The results obtained also demonstrate the need for adopting a flexible approach to the evaluation of data.

We believe that the observations of Heat-after-Death are of special significance because they point the way towards the construction of energy efficient systems based on electrochemical charging. One of the shortcomings of research hitherto has been the failure to integrate this phenomenon into the methodology. We note also that any future work on this aspect should take due account of the long term maintenance of enthalpy production at zero enthalpy input provided the systems are maintained at elevated temperatures (22).

APPENDIX A. [k_R'] HEAT TRANSFER COEFFICIENT FORMAT

Added by Jed Rothwell in 2018

Fleischmann used the designation [k_R'] where R is the radiative heat transfer coefficient, with 2 or 3 subscripts: [k_R'] $_{i, j, l}$. The subscripts mean:

i Method of analysis. 1=Differential; 2=Backward integration; 3=Forward integration

j When present: Time period of measurement cycle. When there are only two subscripts this term is not included.

- j=5, times somewhat above the origin
- j=6, times somewhat above t_1 [application of calibration pulse]
- j=7, times somewhat above t_2 [cessation of calibration pulse]
- j=8, combination of times for j=6 and j=7

l Indicates 1=Lower bound; 2=True

Thus:

[k_R']$_{11}$ indicates: Differential, Lower bound.
[k_R']$_{262}$ indicates: Backward integration; Time period 6; True value.

A single bar over the k_R' term indicates this is an 11-point average value, where values are measured every 5 minutes (55 minutes):

$\overline{k_R'}$

The double bar, used in other documents, indicates a double average; that is, 6 of the 11-point averages combined (6 × 55 = 330 minutes total):

$\overline{\overline{k_R'}}$

Source: Miles, M., M. Fleischmann, and M.A. Imam, *Calorimetric Analysis of a Heavy Water Electrolysis Experiment Using a Pd-B Alloy Cathode* 2001, Washington: Naval Research Laboratory, pages 4-5. Averages described on page 12. http://lenr-canr.org/acrobat/MilesMcalorimetrd.pdf

APPENDIX B. MELVIN MILES DISCUSSES FLEISCHMANN'S CALORIMETRY IN RETROSPECT

Comments made in 2018

The advantages of backward integration are that time zero is the midpoint of the two day cycle, and extrapolations to zero time are much shorter than for forward integrations hence smaller errors. These extrapolations to zero time give the y-intercept which is the value for k_R' at that point in time. This straight-line treatment of the integrated data also gives the cell heat capacity (C_pM) from the slope of the straight line.

The x and y axes in these graphs both have the same units as k_R' (WK^{-4}) and have a slope of about 1.0. This was never explained by Martin, and it took me some time to finally understand his methods. In earlier publications using integrations, the slope was much smaller ($1.00/C_pM$). Martin later made a substitution using an estimated value for the cell heat capacity (C_pM'). The closer his estimate was to the correct C_pM, then the closer the slope was to exactly equal 1.0000. I had people suggest that Martin did not understand the use of significant figures because he reported k_R' values using five significant figures. From Martin's method, all five numbers reported are significant. The C_pM values are less accurate and were generally reported using 3 or 4 significant figures.

Martin stressed the use of the lower bound method as the first step in any analysis of the calorimetric data from isoperibolic calorimetry. If there is no excess heat in the experiment, then there will be nearly constant lower bound heat transfer coefficients obtained throughout the experiment which should be about the same as the true heat transfer coefficient (cell constant). If the experiment shows excess power effects, then the lower bound heat transfer coefficients will show changes. The lower bound value will decrease when the excess power in the cell increases. If there are time periods with no excess power, then the lower bound coefficients should be nearly the same as the true coefficient.

In conclusion, I think Martin Fleischmann was the only one capable of squeezing so much information out of the poor little electrochemical Dewar cell.

Further reading:

Fleischmann, M. and S. Pons. *Calorimetry of the Pd-D_2O System: from Simplicity via Complications to Simplicity*. in *Third International Conference on Cold Fusion, "Frontiers of Cold Fusion"*. 1992. Nagoya Japan: Universal Academy Press, Inc., Tokyo, Japan. http://lenr-canr.org/acrobat/Fleischmancalorimetra.pdf

M., M. Fleischmann, and M.A. Imam, *Calorimetric Analysis of a Heavy Water Electrolysis Experiment Using a Pd-B Alloy Cathode* 2001, Washington: Naval Research Laboratory, pages 4-5. http://lenr-canr.org/acrobat/MilesMcalorimetrd.pdf

Developments in Electrochemistry - Science Inspired by Martin Fleischmann, ed. D. Pletcher, Z.Q. Tian, and D.E.G. Williams. 2014: Wiley, chapter 13.

References

1) Information about this Report is available in Infinite Energy 30(2000)
2) Hand book "ICARUS" Isoperibolic Calorimetry; Acquisition, Research. and Utilities System "Version 1, Low Power Measuring System for Three Cells, December (1993), Technova Inc., 13th Floor, Fukoku Seimei Building, 2-2-2 Uchisaiwai-cho, Chiyoda-ku, Tokyo 100, Japan.
3) Handbook: "ICARUS 2": Isoperibolic Calorimetry: Acquisition, Research and Utilities System" Version 2.00 February (1995), Technova Inc., 13th Floor, Fukoku Seimei Building, 2-2-2 Uchisaiwai-cho Chiyoda-ku, Tokyo 100, Japan.
4) Martin Fleischmann and Stanley Pons, Proceedings of the Third International Conference on Cold Fusion, Editor; H. Ikegami, Universal Academy Press, Frontiers of Science Series no 4 (FSS-4), ISSN 0915-8502, ISBN 4-946443 -12-6 (1993) 118.
5) Martin Fleischmann and Stanley Pons, Phys. Lett. A 176 (1993) 118
6) S. Pons and M. Fleischmann, Proceedings of the Fourth International Conference on Cold Fusion, EPRI TR-104188-V2 (1994) page 8-1
7) S. Pons and M. Fleischmann, Trans. Fusion Technology, 26 (1994) 87
8) Martin Fleischmann, Proceedings of the Seventh International Conference on Cold Fusion, ENECO Inc., Salt Lake City, U.S.A. (1998) 119
9) M.H. Miles, M.A. Imam and M. Fleischmann, to be published
10) M. Fleischmann, S. Pons, Monique Le Roux and Jeanne Roulette, Proceedings of the Fourth International Conference on Cold Fusion, EPRI TR-I04188-VI (1994) page 1-1
11) M. Fleischmann, S. Pons, Monique Le Roux and Jeanne Roulette, Trans. Fusion Technology, 26 (1994) 323.
12) M. Fleischmann, Proceedings of the Fifth International Conference on Cold Fusion, IMRA Europe SA, Valbonne, France (1995) 140
13) Report on the First Set of Experiments carried out under the NEDO / NHE Project at the Sapporo Laboratories, June 1994
14) Second Report on the Experiments carried out under the NEDO / NHE Project at the Sapporo Laboratories, December (1994)
15) S. Pons and M. Fleischmann, Trans. Fusion Technology 26 (1994) 87
16) M.H. Miles, B.F. Bush and K.B. Johnson, "Anomalous Effects in Deuterated Systems", NA WCW PNS TP 8302, September (1996)
17) M.H. Miles and K.B. Johnson, in "Progress in New Hydrogen Energy", Editor: M. Okamoto, Proceedings of ICCF-6, Vol. 1 (1996) 20
18) M.H. Miles, Proceedings of ICCF-8, (2000)

19) M.H. Miles, M. Fleischmann and M.A. Imam, “Calorimetric Analysis of a Heavy Water Electrolysis Experiment Using a Pd-B Alloy Cathode”, NRL Report (in press)
20) S. Szpak, M. Fleischmann, M.H. Miles, S.R. Chubb and T.A. Chubb, “The behaviour of the Pd / D System: A Decade of Research at Navy Laboratories” NRaD Report (in press)
21) Toshiya Saito, Masao Sumi, Naoto Asami and Hideo lkegami, Proceedings of the Fifth International Conference on Cold Fusion, IMRA Europe S.A., Valbonne, France (1995) 105
22) G. Mengoli, M. Bernardini and G. Zannoni, J. Electroanal. Chern., 444 (1998) 155

Figures

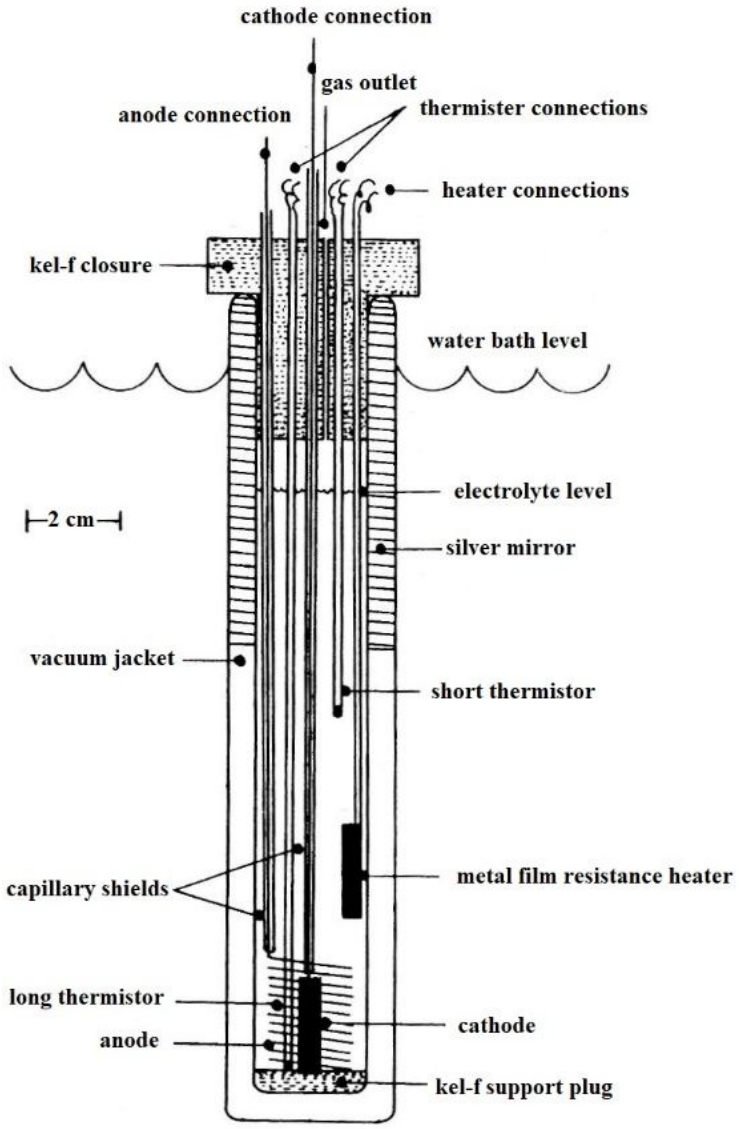

Figure 1. ICARUS-1 type cell; diagram approximately to scale

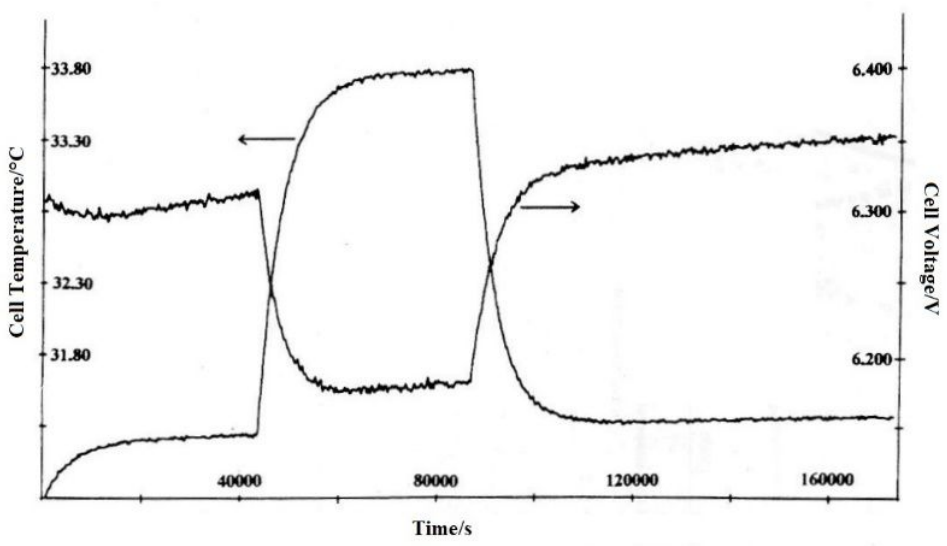

Figure 2. Raw data for days 5 and 6 of experiment FP2-950-6203-5661

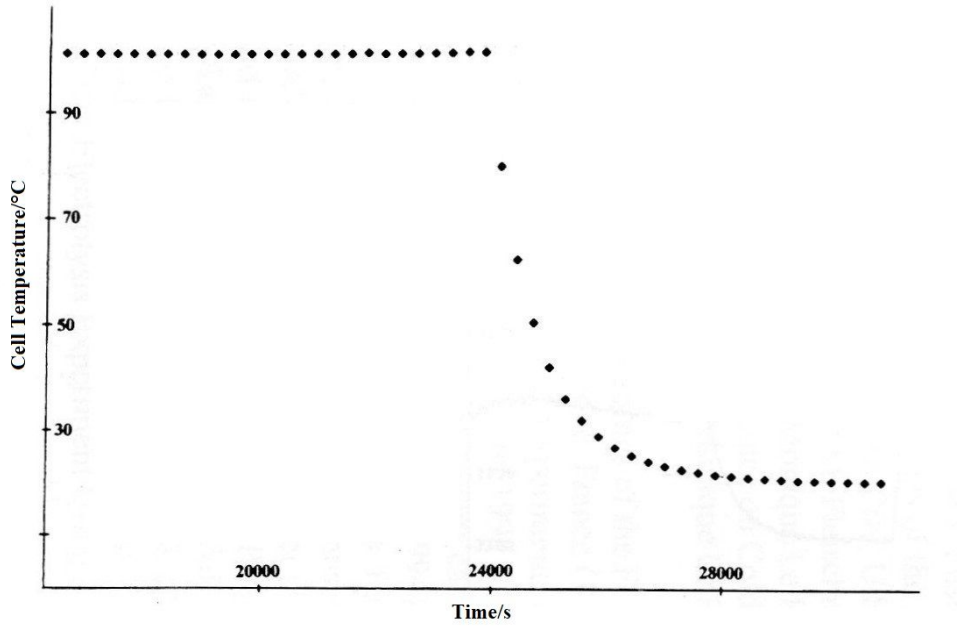

Figure 3. Cell temperature ("Long thermistor") for FP2-950-6203-5661; dryness at 23,700 s

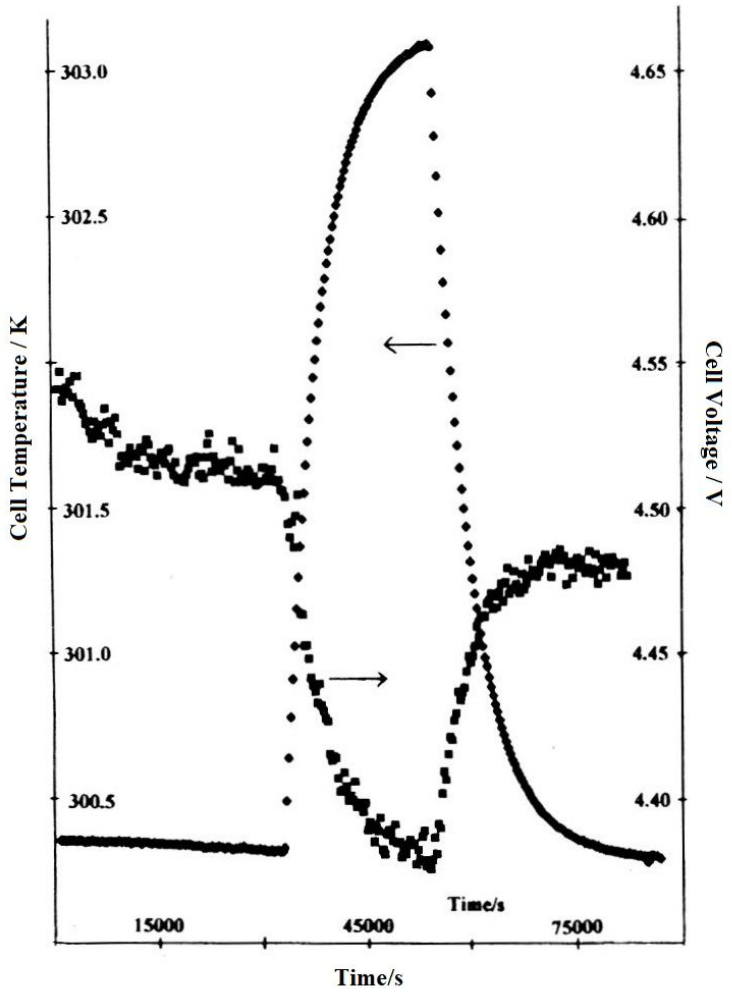

Figure 4. Cell temperature and cell voltage for day 3 of FP 2-97120402-M7C2

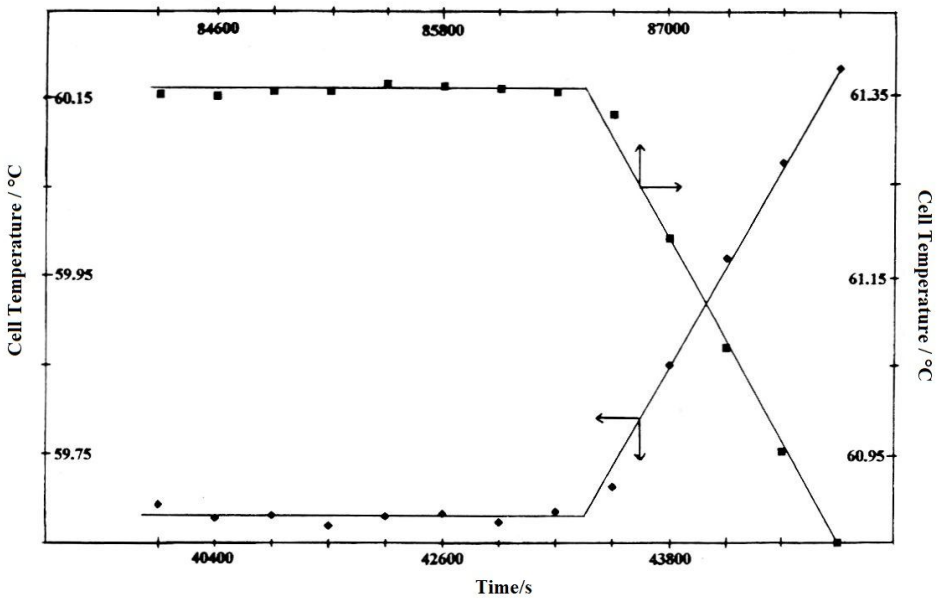

Figure 5. That means cell temperatures four days 13 to 28 in the region of application and cessation of the calibration pulses

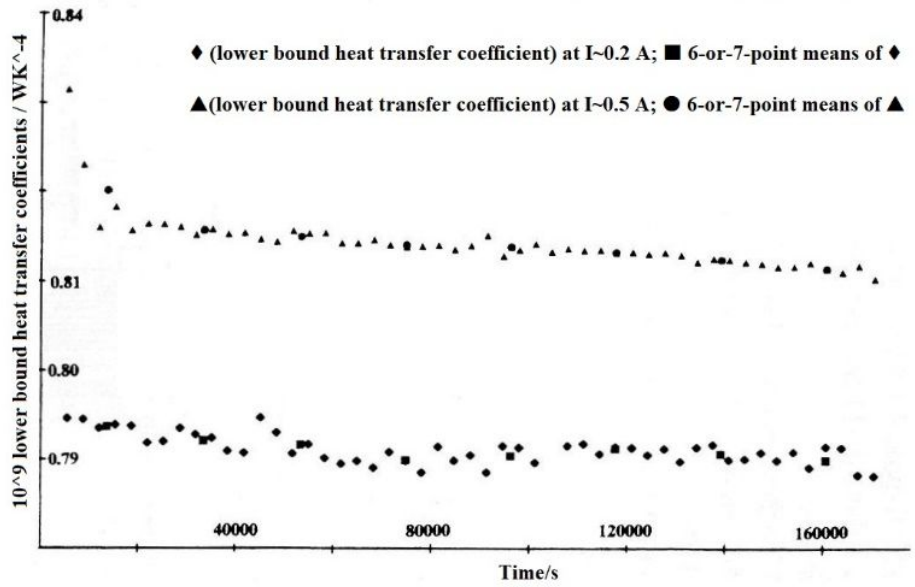

Figure 6. The mean lower bound heat transfer coefficients for Days 9 to 10 and 11 to 12; water equivalent = 490 JK^1

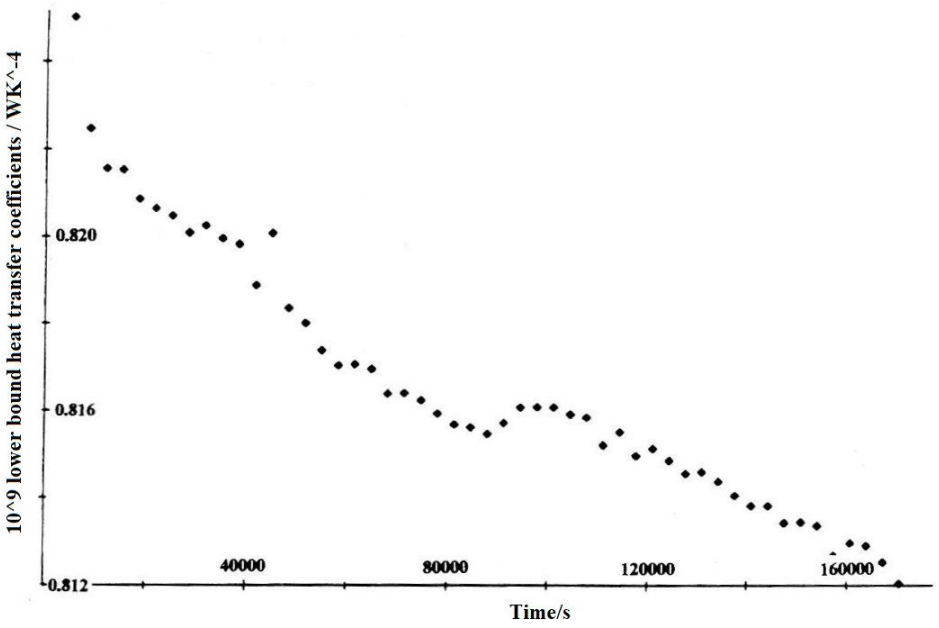

Figure 7. The central region four days 13 to 26

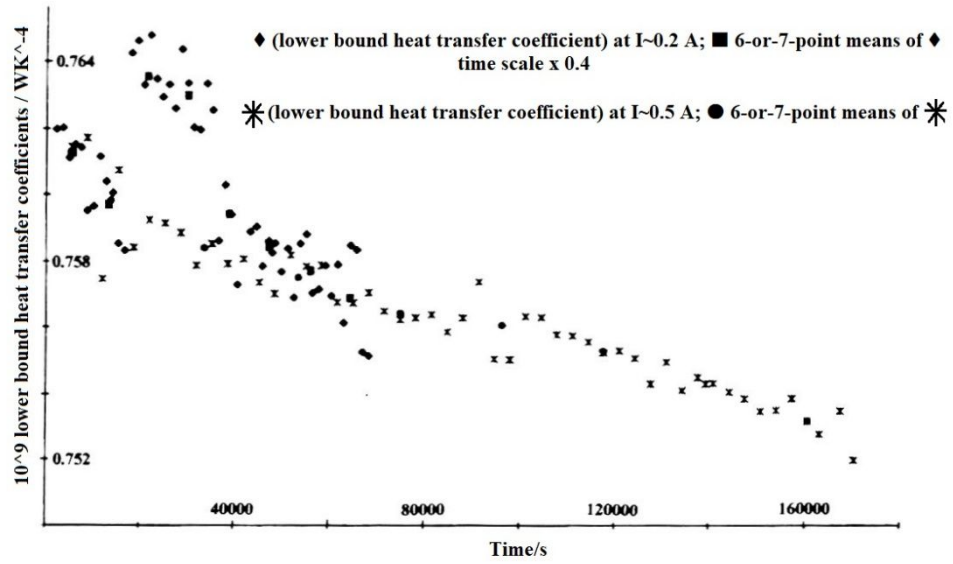

Figure 8A. The mean lower bound heat transfer coefficients for days 92 10 and 11 to 12; ohm resistance in current leads.

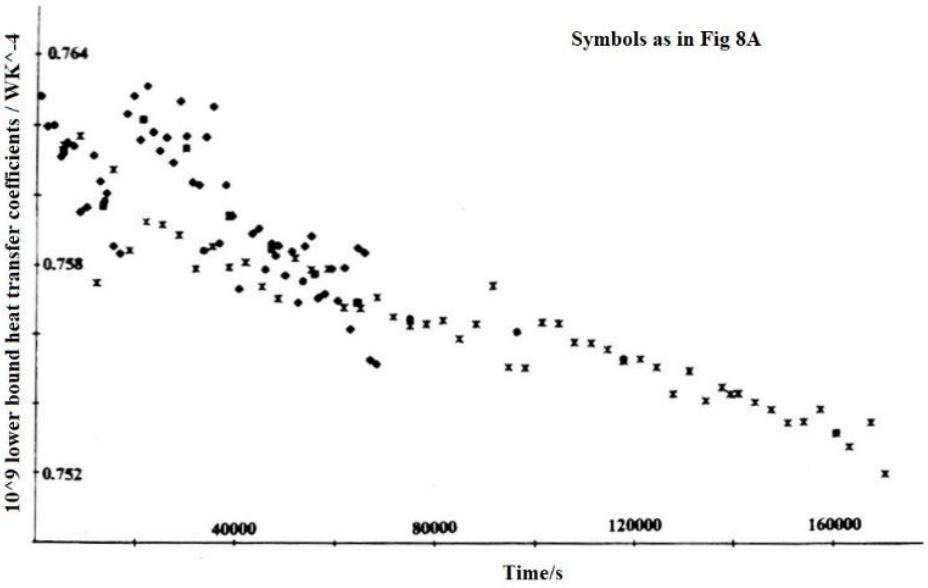

Figure 8B. The mean lower bound heat transfer coefficients for days 9 to 10 and 11 to 12; 1 Ohm resistance in current and heater leads.

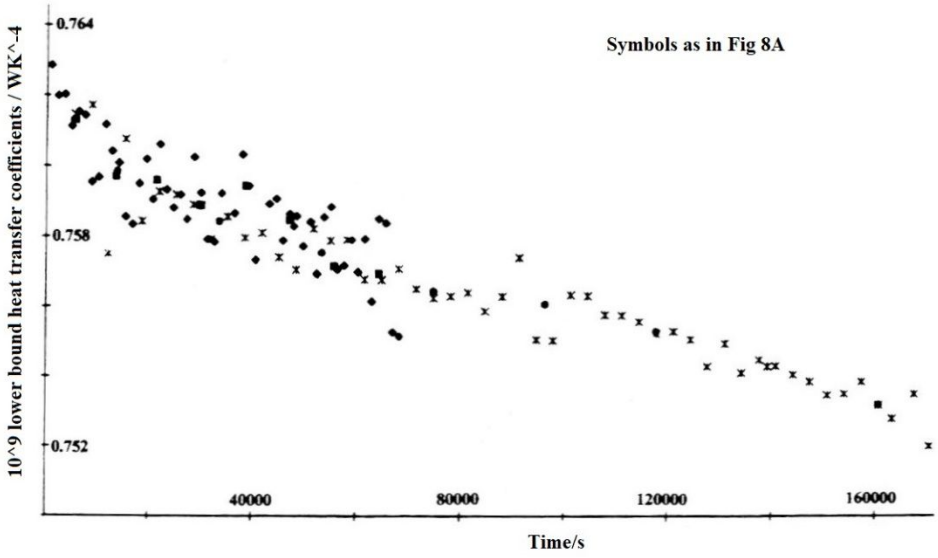

Figure 8C. The mean lower bound heat transfer coefficients for days 9 to 10 and 11 to 12; 1 Ohm resistance in current and 2.5 Ohm resistance in heater leads

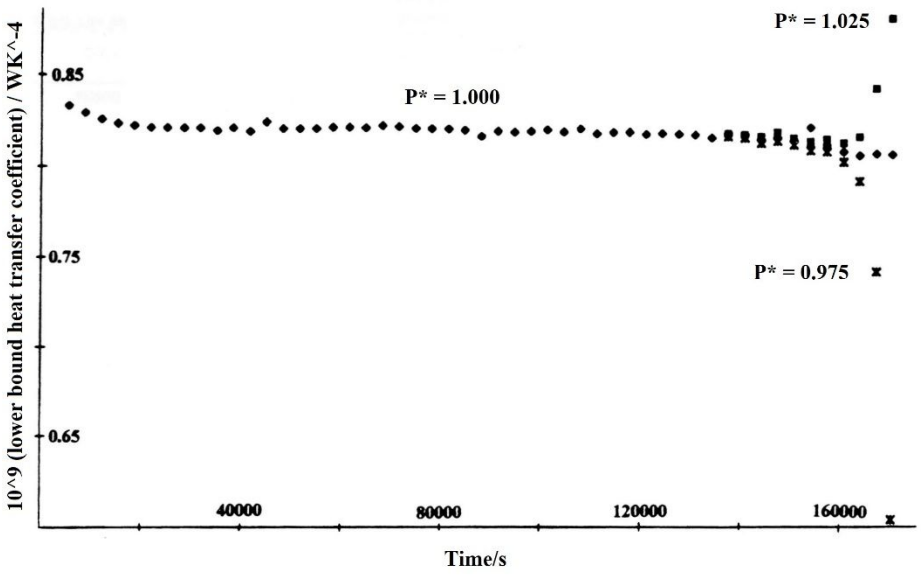

Figure 9. The lower bound heat transfer coefficient for Days 27 to 28 at P* shown

	DATA AS GIVEN		DATA ALLOWING FOR DISSIPATION OF POWER IN CELL LEADS	
ENTHALPY INPUT	403,921 J		392,071 J	
ENTHALPY OUTPUT	235,567 J		225,476 J	
ENTHALPY FOR HEATING CELL	522 J		522 J	
ENTHALPY AVAILABLE FOR EVAPORATION	168,354 J		166,073 J	
	5 MOLES D_2O	6 MOLES D_2O	5 MOLES D_2O	6 MOLES D_2O
ENTHALPY REQUIRED FOR EVAPORATION OF	208,163 J	250036 J	208,363 J	250,036 J
EXCESS ENTHALPY REQUIRED	40,531 J	82.204 J	42,290 3	83,963 J
MEAN RATES OF EXCESS ENTHALPY GENERATION	1.71 W	3.46 W	1.78 W	3.54 W
MEAN SPECIFIC RATES OF EXCESS ENTHALPY GENERATION	43.05 W	88.1W	45.3 W	90.1 W

Figure 10. The enthalpy balances for t < 23,700 of day 29

COLLIGATIVE PROPERTIES OF SOLUTIONS	
INFORMATION REQUIRED	COMMENTS
SOLUBILITY	KNOWN
BOILING POINT	KNOWN
ATMOSPHERIC PRESSURE	NOT KNOWN
	PRESSURE SENSOR
	DISCONNECTED?
REFLUX RATIO	NOT KNOWN
POSITION OF TEMPERATURE SENSOR	NOT KNOWN
CONCENTRATION	NOT KNOWN
VOLUME OF ELECTROLYTE	NOT KNOWN
DEVIATIONS FROM IDEALITY	NOT KNOWN

Figure 11. Information required for the evaluation of the rates of excess enthalpy generation on Day 29

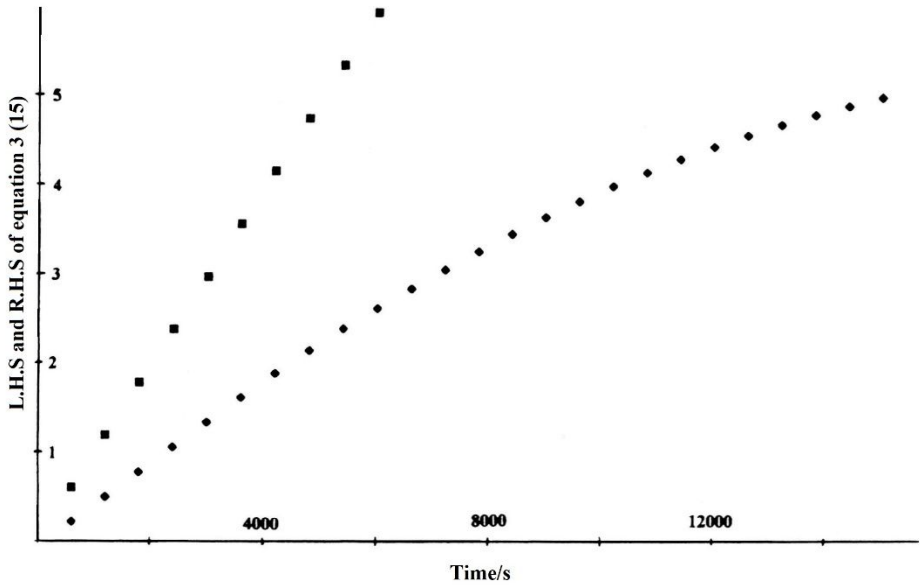

Figure 12. Cooling curves on day 29; ■ prediction for Q = 0; ♦ behaviour derived from Fig. 4

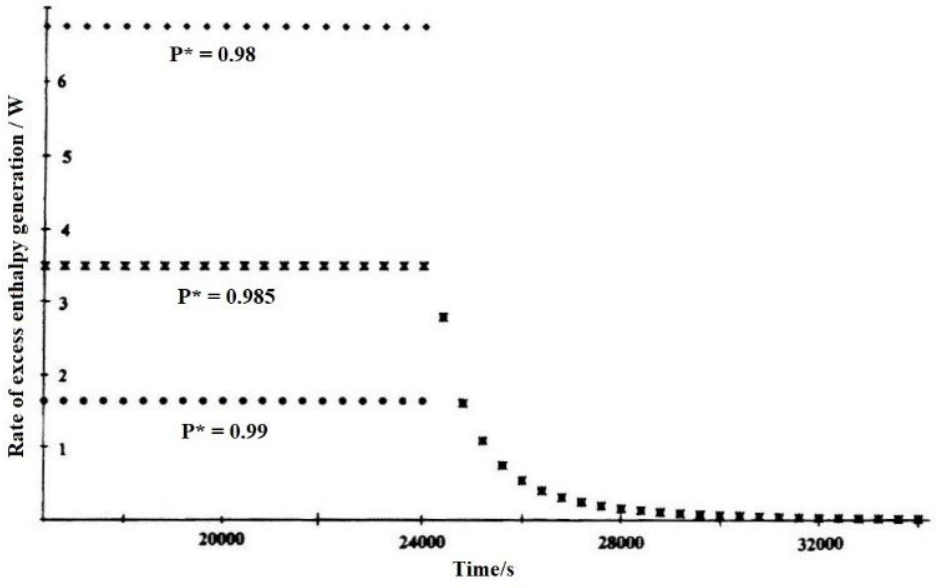

Figure 13. The rate of excess enthalpy generation on day 29

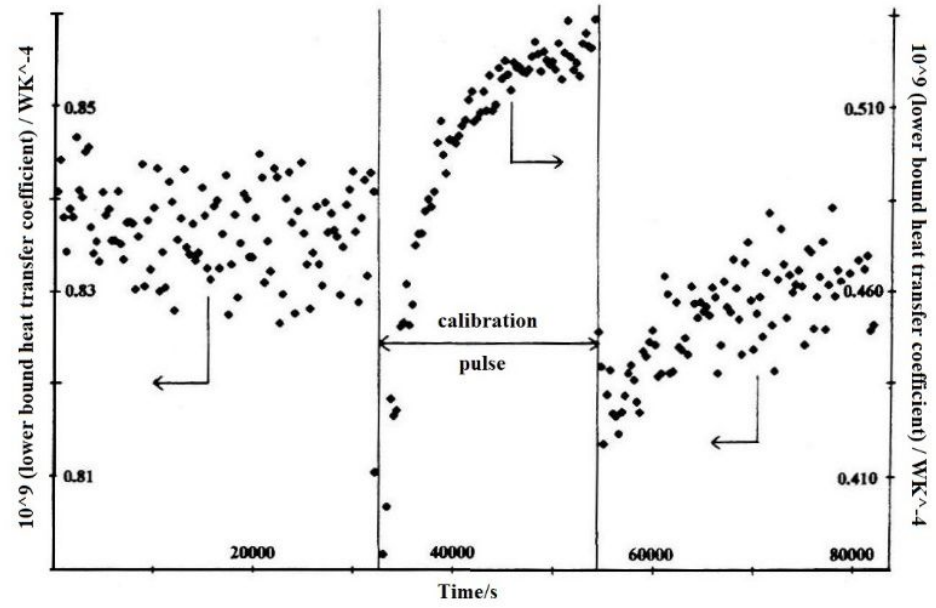

Figure 14. Lower bound heat transfer coefficient for Day 3: NHE Analysis

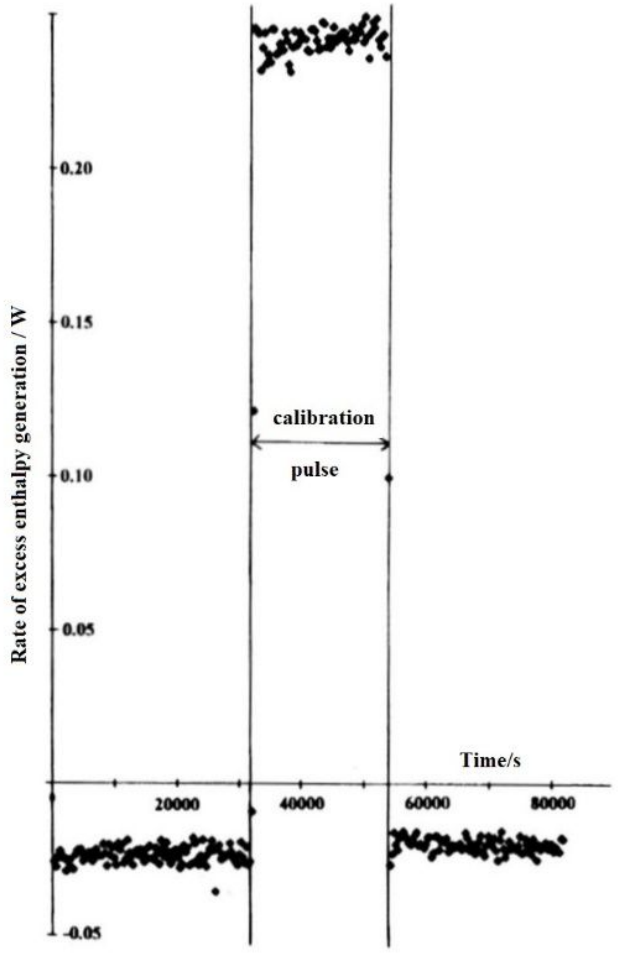

Figure 15. The rate of excess enthalpy generation; NHE Analysis

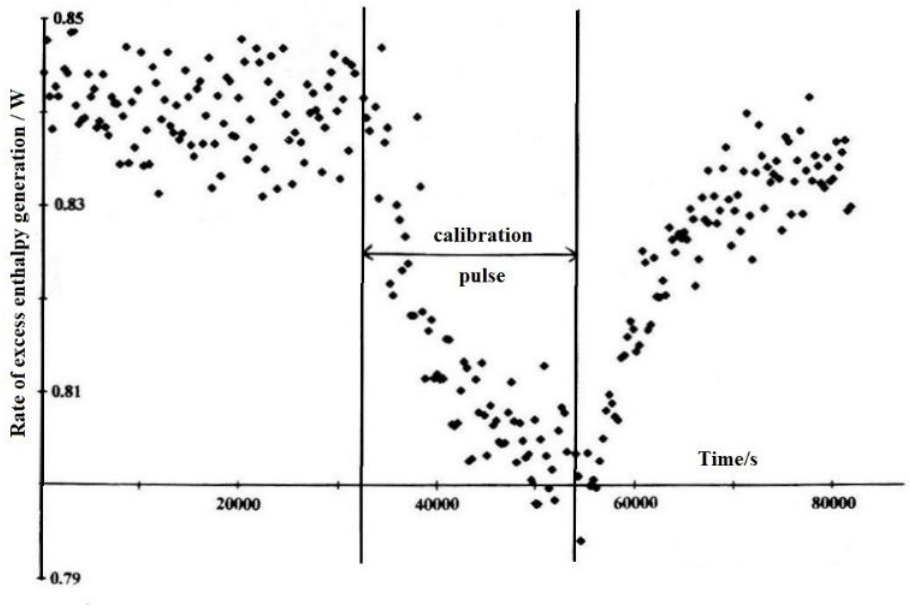

Figure 16. Lower bound heat transfer coefficient for Day 3: ICARUS Analysis

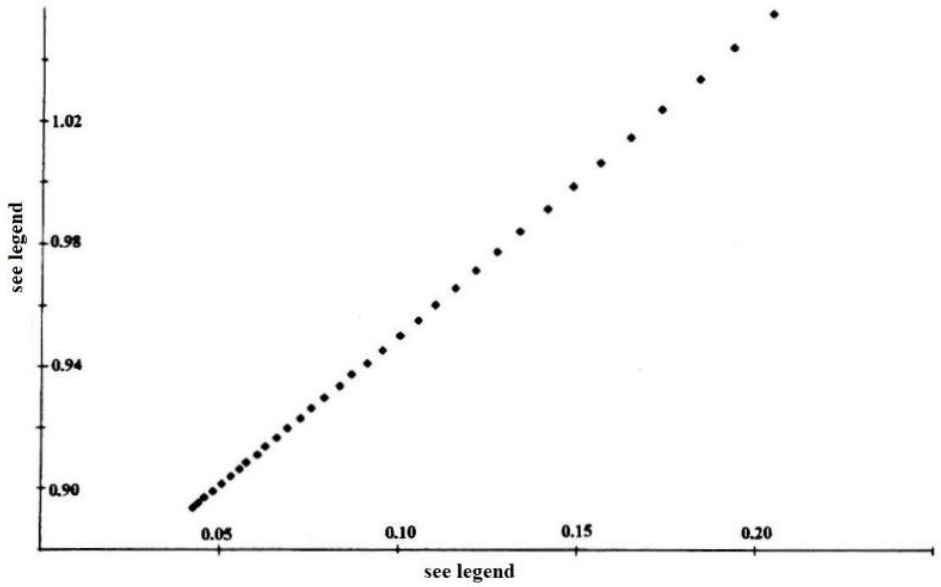

Figure 17. Evaluation of $[k_R']_{352}$ and of the water equivalent for the third measurement cycle and with correction for the effects of "positive feedback"

$$\text{Ordinate} = [k_R']_{352} + \frac{\int_{t_1}^{t} \text{net enthalpy } d\tau - [\text{net enthalpy input } (t_1)][t - t_1]}{\int_{t_1}^{t} f_2(\theta) d\tau}$$

$$\text{abscissa} = \frac{\text{water equivalent } \times \ [\Delta\theta(t) - \Delta\theta(t_1)]}{\int_{t_1}^{t} f_2(\theta) d\tau}$$

Where $f_2(\theta) = [\theta_{\text{bath}} + \Delta\theta(t)]^4 - [\theta_{\text{bath}} + \Delta\theta(t_1)]^4$

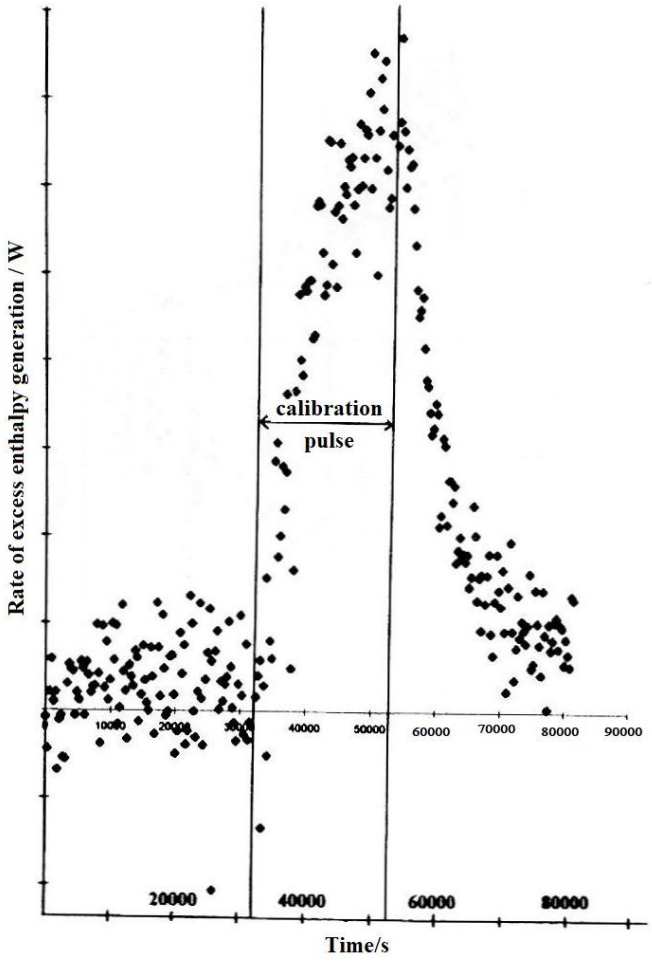

Figure 18. The rate of excess enthalpy generation on Day 3: ICARUS Analysis

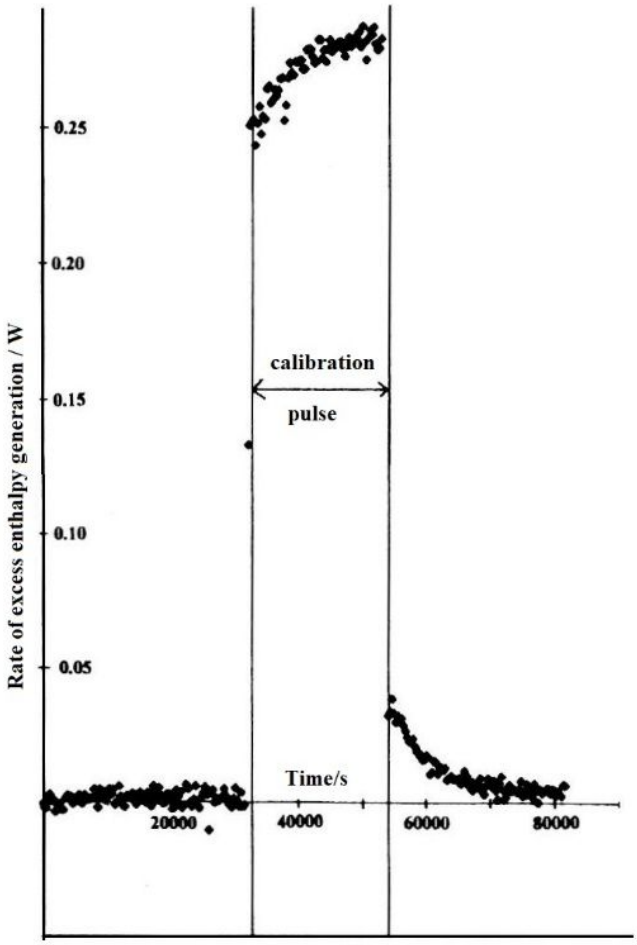

Figure 19. Rate of excess enthalpy generation on day three ICARUS Analysis by analogy to NHE procedure

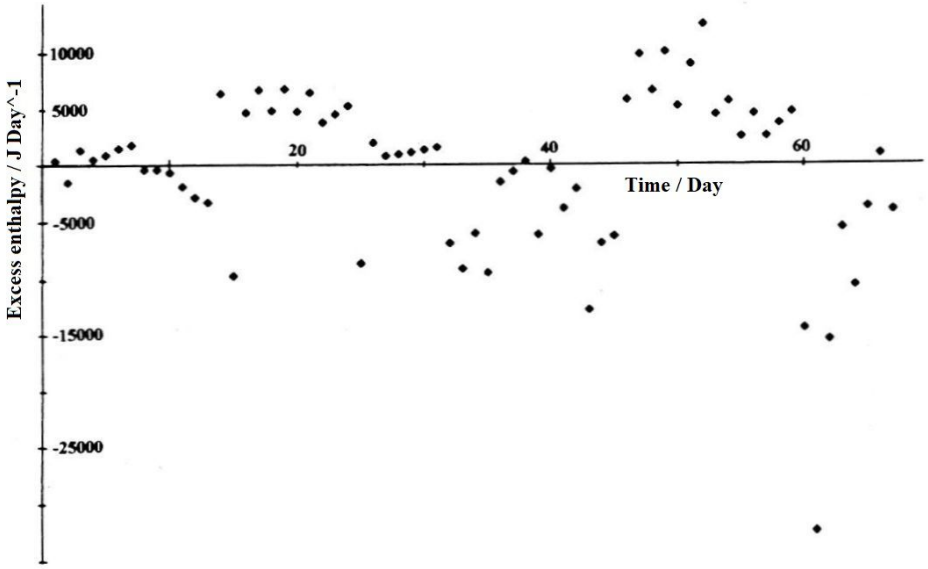

Figure 20. Excess enthalpies using NHE procedure

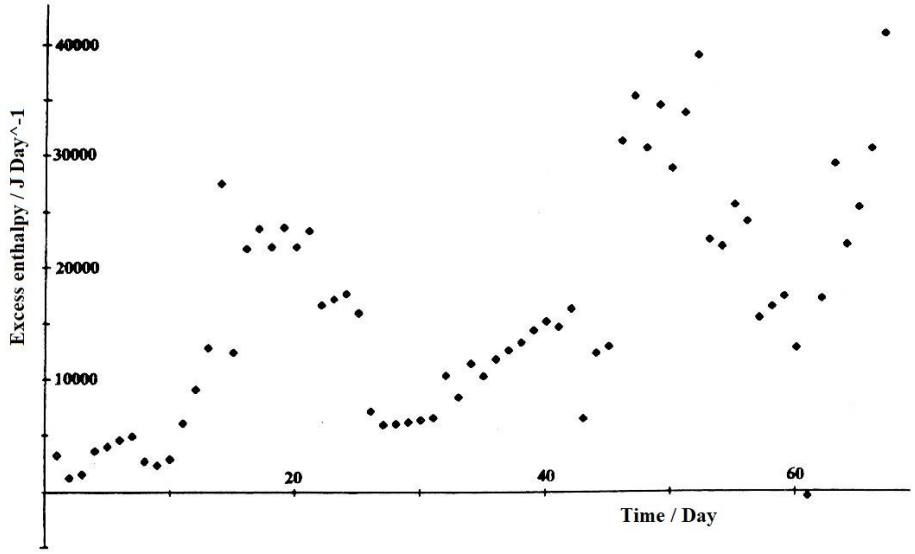

Figure 21. Excess enthalpies using ICARUS procedure

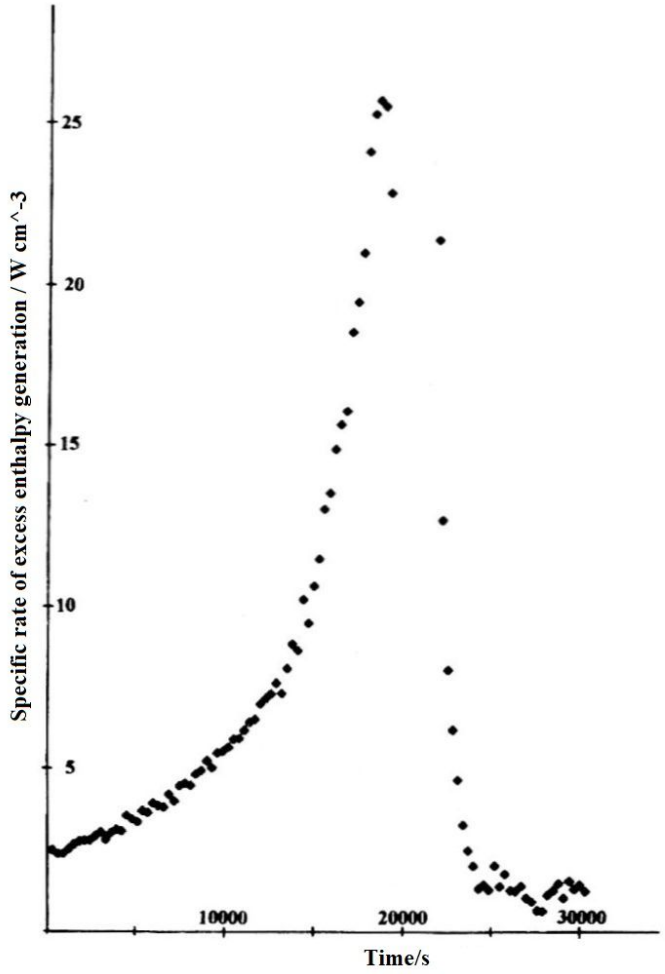

Figure 22. Specific rate of excess enthalpy production on Day 29 for 0 < t <21,000 s < t < 30,000 s